

Duncan Axisa*, Amit Teller, Roelof Bruintjes, Dan Breed, Roelof Burger
National Center for Atmospheric Research (NCAR), Boulder CO USA

Don Collins
Texas A&M University (TAMU), College Station TX USA

1. INTRODUCTION

In recent years, a considerable effort has been made to understand the impact of varying aerosol properties and concentration on cloud properties. Under almost all environmental conditions, increased aerosol concentrations within polluted air masses will enhance cloud droplet concentration relative to that in unperturbed regions. Although there is little debate regarding this rather straightforward impact, extrapolation to the resulting changes in cloud lifetime, dynamical behavior, and precipitation production is challenging. The expectation that high concentrations of smaller droplets will decrease coalescence efficiency, and therefore rainout, is supported by analysis of satellite images that clearly show altered cloud properties downwind of isolated pollution sources. However, observation of the result of increased aerosol concentration is not easily related to a mechanistic description of the responsible microphysical processes.

In order to quantify this aerosol effect on clouds and precipitation, field campaigns have been launched in Istanbul Turkey and central Saudi Arabia as part of Precipitation Enhancement Feasibility Studies. This paper presents aircraft data from Istanbul and central Saudi Arabia for case study days when air pollution and mineral dust was predominant in the region.

Sophisticated aircraft platforms were used in Istanbul Turkey and Riyadh Saudi Arabia to conduct atmospheric measurements of aerosol and cloud properties. The aerosol and cloud physics research aircraft in Istanbul was operated by Seeding Operations and Atmospheric Research (SOAR). In Riyadh two research aircraft, one cloud physics aircraft and one aerosol aircraft, were operated by Weather Modification Incorporated (WMI). For the cases presented here, the SOAR and WMI aerosol research aircraft were similarly equipped with common instrumentation in each platform. Both aircraft had the capability of measuring the size distribution of aerosols ranging from 0.01 μm to 3 μm . The Differential Mobility Analyzer (DMA) measures

aerosols from 0.01 μm to 0.4 μm while the PMS Passive Cavity Aerosol Spectrometer Probe (PCASP) measures aerosols from 0.1 μm to 3 μm . Both aircraft were equipped with the DMT Cloud Condensation Nucleus (CCN) counter. The SOAR aircraft was equipped with the DMT Cloud Droplet Probe (CDP) that measures cloud droplets from 2 μm to 50 μm and the DMT Cloud Imaging Probe (CIP) that measures cloud hydrometeors from 25 μm to 1550 μm . The WMI aircraft was equipped with the PMS Forward Scatter Spectrometer Probe (FSSP) that measures cloud droplets from 3 μm to 47 μm . The WMI cloud physics aircraft was equipped with the Cloud Aerosol and Precipitation Spectrometer (CAPS) probe that measures aerosols and cloud hydrometeors ranging from 0.3 μm to 1550 μm .

2. ISTANBUL CASE STUDY

2.1 Case study: 20 March 2008

On the 20th March 2008 a surface cold front was to the south of Istanbul. The cold air was confined to 700m above sea level on the Istanbul 12Z sounding. Istanbul airport reported light rain showers overnight up to 04:20Z with up to 24 mm of precipitation measured between 19th March 06Z and 20 March 06Z. The SOAR research aircraft conducted measurements in areas identified in Figure 1. The orange track is the aircraft track and the blue, green and red arrows are HYSPLIT back trajectories.

Time (GMT)	Altitude (m)	Temp ($^{\circ}\text{C}$)	Aerosol conc dN/dlogD_p (cm^{-3})	Max CDP conc (cm^{-3})
094816 094936	climb from 400 to 650	5.5 to 3.7		1014.3
100714 101548	1056	3.6	643.5	
102533 103533	920	2.0		299.8
112844 113838	1005	4.3	2287.6	
115000 120000	796	3.5		343.9
121718 121839	952	5.3	681.1	
121814 121942	930	4.9		133.8

Table 1: Flight levels with alternating aerosol and cloud measurements on 20th March 2008.

Corresponding author address:

Duncan Axisa,
National Center for Atmospheric Research (NCAR)
PO Box 3000, Boulder, CO 80307.
E-mail: duncan@ucar.edu

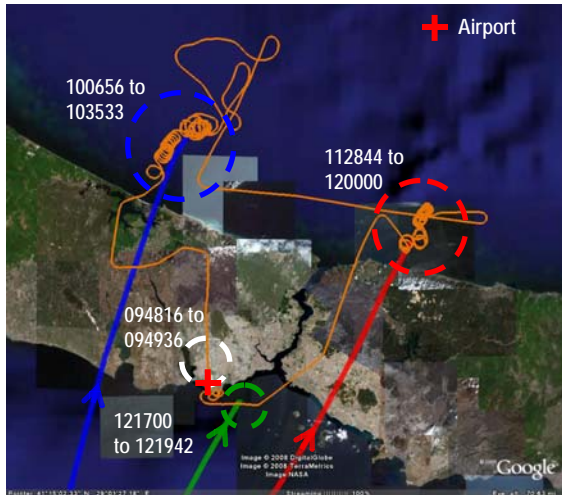


Figure 1: NOAA HYSPLIT 72 hour back trajectories ending near Istanbul at 12UTC on 20 March 2008.

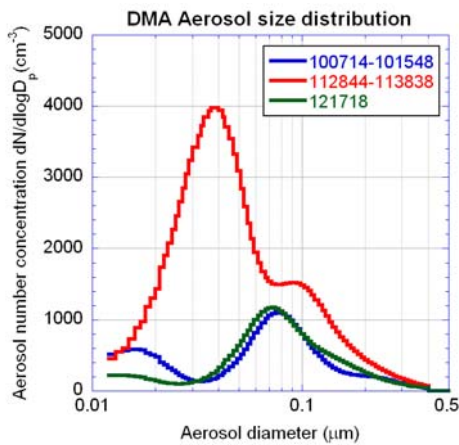


Figure 2: DMA size distributions at each flight leg.

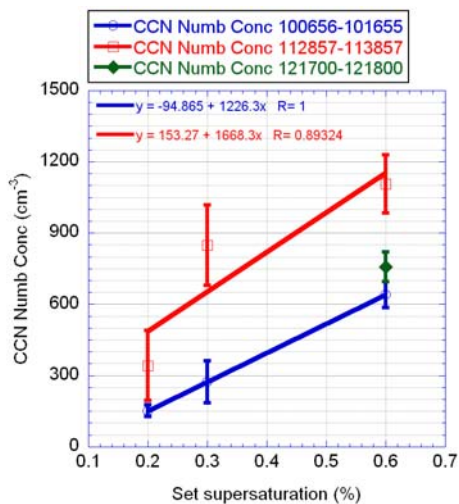


Figure 3: CCN concentrations [cm^{-3}] at 0.2%, 0.3% and 0.6% supersaturation.

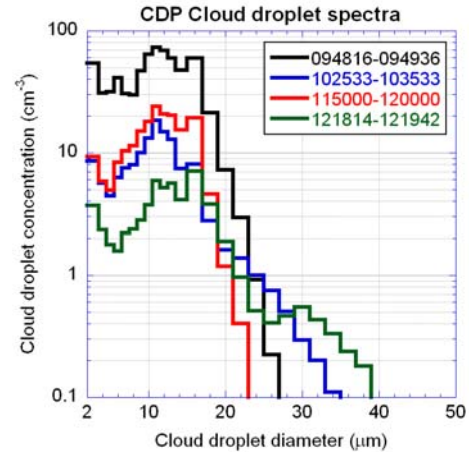


Figure 4: Cloud droplet concentrations [cm^{-3}] averaged over the time interval shown in the legend.

The cloud layer measured was stratiform with tops at about 1km. Table 1 shows the measurement altitudes. The aerosol measurements were taken immediately above the thin stratus cloud layer as cloud bases were below the minimum vectoring altitude.

The aerosol size distribution, the CCN number concentration and the cloud droplet distribution are shown in Figure 2, Figure 3 and Figure 4 respectively. The data were averaged over the time period shown in the legend and correspond to data collected in the areas shown in Figure 1. The aircraft encountered cloudy air almost immediately after takeoff and climb out so no aerosol measurements can be shown below cloud base. DMA and CCN concentrations prior to the takeoff run were too high and are not believed to be representative of aerosol properties at cloud base. The DMA concentrations are shown in units of dN/dlogD_p (cm^{-3}) so that the number of particles within the narrow size interval selected by a DMA is normalized according to the width of the interval. In Figure 2 all three size distributions were measured at an altitude of about 1km, so the difference in concentrations of the three size distributions can be compared directly. It is evident that the aerosol size distribution measured between 11:28:44 and 11:38:38 has an Aitken mode which is much higher than those in the two other measurement periods (10:07:14-10:15:48, 12:17:18-12:18:39). It is believed that this is due to the transport of surface pollution from the heavily populated Istanbul downtown area on the Asian side onto the Black Sea coast where the measurements were made. The most maritime size distribution is measured at 12:18:39. The distribution measured at 10:15:48 has a higher nucleation mode than that measured at 12:18:39. The higher nucleation mode may be attributed to gas-to-particle conversion. The trajectory of the aerosol measured at 10:15:48 is mostly over the outskirts of the European

Istanbul downtown area and in a less populated Istanbul suburb.

Figure 3 shows the CCN concentrations at 0.2%, 0.3% and 0.6% supersaturation. The CCN concentrations measured at 11:38:57 downwind of downtown Istanbul are quite higher than those measured at 10:16:55. CCN measurements on the Sea of Marmara at 12:18:00 were not complete since the aircraft was in sequence for landing at the Istanbul Ataturk Airport. The CCN concentrations at 0.6% supersaturation over the Marmara were quite similar to those measured at 10:16:55 over the European side on the Black Sea coast.

Cloud droplet size distributions were measured in the same area of the aerosol measurements and are shown in Figure 4. Most of the cloud measurements were made at altitude ranging from 0.8km to 1km at the tops of stratus cloud layers. The stratiform cloud had lower bases over the airport (indicated by a red cross in Figure 1) and the aircraft was in cloud during the climb out immediately after takeoff from 09:48:16 to 09:49:36. The cloud droplet size distribution (DSD) during climb out from an altitude of 400m to 650m is shown by the black trace in Figure 4. During the cloud penetration, cloud droplet concentrations in the stratus deck reached 1014 cm^{-3} . Aerosol concentrations on the ground were quite high with CCN concentrations reaching 4000 cm^{-3} at 0.3% supersaturation (not shown here). Figure 4 shows the black trace is the most polluted DSD with high droplet concentrations and a narrow drop size distribution reaching a maximum cloud droplet diameter of $27 \mu\text{m}$. The aircraft took off on a northerly heading. The surface winds were light and northeasterly becoming light and southerly at 1km. The aircraft conducted cloud measurements over the Black Sea coast on the European side (blue DSD, 10:25:33-10:35:33) followed by cloud measurements on the Asian side (red DSD, 11:50:00-12:00:00). The DSD on the European side are quite broader than those measured during the climb out with cloud droplets diameter reaching $35 \mu\text{m}$. A narrowing of the DSD is observed on the Asian side over the Black Sea coast. In this area downwind of downtown Istanbul, the cloud droplet diameter reached $23 \mu\text{m}$. Cloud DSD broadening is then observed as the aircraft penetrates cloud on the Marmara coast while on approach to the airport. Here the cloud droplet diameter reaches $39 \mu\text{m}$.

This case presents data showing that background aerosol concentrations after an extended period of precipitation reach a total aerosol number concentration of 681.1 cm^{-3} with CCN concentrations of around 600 cm^{-3} at 0.6% supersaturation. The aerosol is polluted by the heavily populated Istanbul downtown area causing an increase in the aerosol concentration up to 2287.6 cm^{-3} . The CCN concentration increases to around 1000 cm^{-3} at 0.6% supersaturation and a narrowing of the drop size

distribution is observed from a maximum drop size diameter of $39 \mu\text{m}$ in relatively clean conditions to $23 \mu\text{m}$ in the polluted plume.

3. SAUDI ARABIA CASE STUDY

3.1 Case study: 9 April 2007

On 9 April 2007 a severe dust storm hit Riyadh Saudi Arabia that reduced the visibility to a fraction of a mile. On this day, the Aerosol Optical Depth (AOD) was 0.9, which is very high for this region. The Angstrom exponent was about 0.1 suggesting that large particles (desert dust) were dominant.

Convection occurred first in the Qassim area by 0800Z with storms forming in the Riyadh area later that morning. The day was characterized by intense convection and large scale organization, with lines of thunderstorms forming and moving through Qassim and Riyadh into the night. Cloud tops extended to 11 km, and lightning was frequent from several storms. The boundary layer supported the development and propagation of gust fronts ("haboobs"), which affected operations at King Khaled International Airport. Very gusty winds were associated with thunderstorm outflows. Visibility became extremely poor with gusty winds and blowing dust.

The aircraft took off at 1157Z. The visibility was so poor that the cloud bases were not visible and the aircraft flew through cloud occasionally while climbing. At 18000 ft, the crew had a good view of the cloud tops. After profiling the cloud from 18000 ft down to 14700 ft, an aerosol profile was flown all the way to the airport. Below cloud base the visibility was on the order of a few feet and the aircraft was flying in a cloud of dust. The aircraft wing tip was visible but no cloud features could be identified even when flying just below cloud base. The control tower at King Khalid International airport reported zero horizontal visibility at the airport. The aircraft descended at 500 ft/min down to 9800 ft where the ground was visible vertically downwards.

Figure 5 and 6 show the aerosol profile data during the ascent and the descent, respectively. During the ascent, the mean boundary layer PCASP coarse mode concentration (1.2 to $3 \mu\text{m}$) was 13.2 cm^{-3} with a maximum of 183 cm^{-3} . During the descent the mean coarse mode concentration was 42.2 cm^{-3} with a maximum of 308 cm^{-3} . These PCASP coarse mode concentrations were the highest encountered throughout the campaign. Figure 7 shows the aerosol size distributions averaged over a 9 minute period at 10000ft. Figure 7 shows a peak in sub-micron aerosol concentration at $0.04 \mu\text{m}$. The aerosol concentrations from $0.5 \mu\text{m}$ to $3.0 \mu\text{m}$ are flat at around 50 cm^{-3} to 100 cm^{-3} . Figure 8 shows increasing values in the volume distribution, reaching a peak of $800 \mu\text{m}^3 \text{ cm}^{-3}$. Analysis of measurements at 6000ft averaged over 9 minutes show similar aerosol

conditions. The average mode in the sub-micron range shifted to $0.1 \mu\text{m}$, but the super-micron aerosol distribution was relatively unchanged (not shown). At 4100ft, 7 minute averaged aerosol concentration increased significantly but the size distribution shape remained the same (not shown). This indicates that the aerosol concentrations below the cloud bases are mostly homogenous and from dust of the same source.

Calculations for total aerosol number concentrations at 10000 ft (1309Z to 1318Z) indicate that the total average sub-micron ($0.0124 \mu\text{m} >x>0.9 \mu\text{m}$) aerosol concentration is equal to 1629.5cm^{-3} and that of super-micron ($0.9 \mu\text{m} >x>3.0 \mu\text{m}$) aerosol concentration is equal to 38.1cm^{-3} .

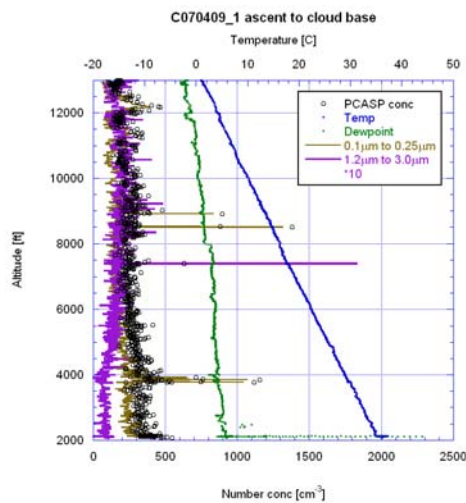


Figure 5: Aerosol profile during ascent to cloud base. Total, fine mode and coarse mode PCASP concentrations are shown.

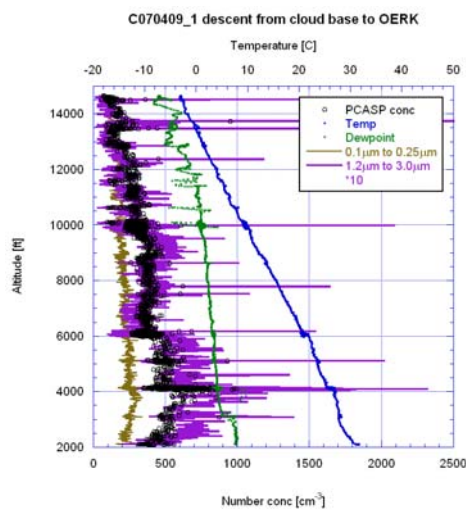


Figure 6: Same as in Figure 5 but for the descent.

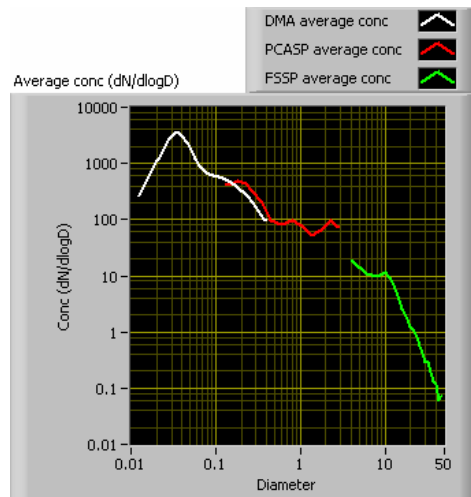


Figure 7: Aerosol size distributions averaged over the time period 13:09-13:18 at 10000ft. Diameter is in μm .

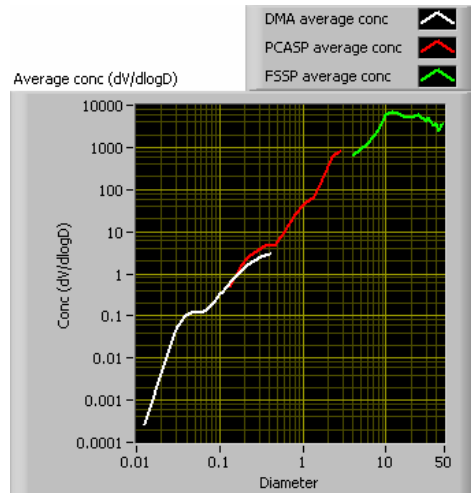


Figure 8: Same as in Figure 7 but for volume distribution [$\mu\text{m}^3\text{cm}^{-3}$]. Diameter is in μm .

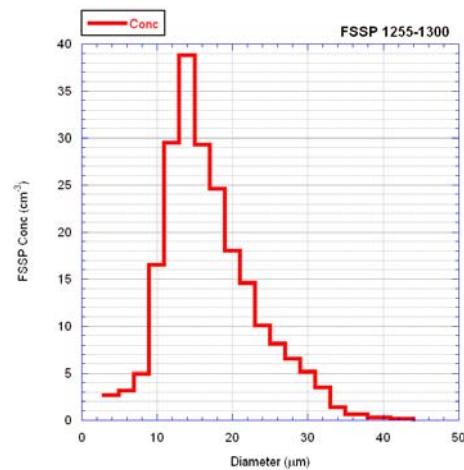


Figure 9: FSSP cloud droplet concentration [cm^{-3}].

The CCN concentrations are calculated from the DMA as the DMT CCN counter was not working on this day. CCN concentrations ranged from around 162.5 cm^{-3} to 380.3 cm^{-3} from 6000 to 10000ft. At 4100ft the CCN concentrations increased to values up to 1134.5 cm^{-3} (not shown). This increase in CCN can be attributed to both the increase in sub-micron aerosol concentration (by a factor of 2) and the increase in super-micron aerosol concentration (by a factor of 3). Figure 9 shows the Forward Scatter Spectrometer Probe (FSSP) cloud droplet concentration at clouds base (1255Z-1300Z) reaching a maximum total concentration of 369.8 cm^{-3} .

In most cases during the Saudi campaign, the sub-micron and super-micron mode particle number concentration decreased significantly with altitude. In early spring and during dusty conditions average super-micron aerosol concentrations reach 125 cm^{-3} . In these cases, aerosol size distributions over the range from 0.5 μm to 3.0 μm are flat with 50 cm^{-3} to 100 cm^{-3} particles in each size bin. Volume size distributions reach 800 $\mu\text{m}^3\text{cm}^{-3}$ in the super-micron size range. In winter, aerosol concentrations are relatively low with super-micron aerosol concentrations below 6 cm^{-3} . In the free troposphere above the dust layer a very low super-micron mode particle number concentration was observed (below 0.1 cm^{-3}).

Trajectory analyses show that dusty conditions are caused by altitude-independent trajectories that originate in the Nubian Desert, southern Egypt and northern Sudan. This suggests that the particles in this layer are Saharan dust aerosols. Within this Saharan dust layer the coarse mode particle number concentration remained roughly constant at about 10 cm^{-3} . In the Saudi cases, the relationship between sub-micron aerosol size distributions and CCN concentration seems to be well characterized. As the sub-micron aerosol concentration increases, the measured CCN at 0.4% supersaturation increased. The super-micron aerosol concentration does not exhibit this observed relationship throughout the boundary layer. Super-micron aerosol in the sub-cloud aerosol layer was found to correlate well with the measured CCN concentrations, suggesting that an increase in super-micron aerosol below cloud base increases CCN activation. Closer to the surface, the correlation between super-micron aerosol concentration and measured CCN concentration was not present.

4. CONCLUSION

Cases from Istanbul Turkey and Riyadh Saudi Arabia show the importance of pollution and mineral dust in aerosol size distributions, the formation of CCN and cloud droplets. In Istanbul, increased aerosol concentrations within polluted air trajectories narrow the drop size distributions relative to less polluted regions. In Saudi Arabia, the conditions in which dust

acts as CCN and forms cloud droplets are unclear. Laboratory studies have shown that small amounts of highly soluble components greatly enhance the ability of fine dust to serve as CCN (Kelly et. al, 2007). Since no measurements of dust solubility was planned during these campaigns, it is not possible to draw any further conclusions on the CCN activation of dust aerosol.

5. REFERENCES

Kelly, J. T., C.C. Chuang, A.S. Wexler, 2007. Influence of dust composition on cloud droplet formation. Atmospheric Environment 41 (2007) 2904–2916.